Am J Cancer Res 2022;12(6):2833-2849
www.ajcr.us /ISSN:2156-6976/ajcr0143840

Original Article

CircNRIP1 acts as a sponge of miR-1200 to suppress osteosarcoma progression via upregulation of MIA2

Ruoxuan Hei[1*], Jinnan Chen[1,2*], Xiaojing Zhang[3], Huiqin Bian[1], Chen Chen[1], Xuan Wu[1], Tiaotiao Han[1], Yiming Zhang[4], Junxia Gu[1], Yaojuan Lu[1,5], Qiping Zheng[1,5]

[1]*Department of Hematological Laboratory Science, Jiangsu Key Laboratory of Medical Science and Laboratory Medicine, School of Medicine, Jiangsu University, Zhenjiang 212013, Jiangsu, China;* [2]*Department of Internal Medicine, Rush University Medical Center, Chicago, IL 60612, USA;* [3]*Department of Clinical Laboratory, Shandong Cancer Hospital and Institute, Shandong First Medical University and Shandong Academy of Medical Sciences, Jinan 252117, Shandong, China;* [4]*Department of Orthopedics, Affiliated Hospital of Jiangsu University, Zhenjiang 212000, Jiangsu, China;* [5]*Shenzhen Walgenron Bio-Pharm Co., Ltd., Shenzhen 518118, Guangdong, China.*
[*]*Equal contributors.*

Received April 30, 2022; Accepted May 12, 2022; Epub June 15, 2022; Published June 30, 2022

Abstract: Circular RNAs (circRNAs), a class of non-coding RNAs, play an essential role in embryo development and carcinogenesis, circNRIP1 was recently identified to promote development of multiple human cancers. This study investigated the role of circNRIP1 in osteosarcoma (OS) cells and the potential mechanisms relating to the sponging miRNAs and their target genes. OS cell lines and normal human osteoblasts were grown for qRT-PCR analysis of circNRIP1 expression and functions of circNRIP1 expression in OS cell proliferation, migration, and invasion *in vitro*. Bioinformatics analysis was then performed to predict the sponge miRNA of circNRIP1 and the target gene, which was confirmed by using the dual-luciferase reporter assay. The *in vivo* functions of circNRIP1 was evaluated in OS cell xenograft models, while levels of relevant marker genes were examined using immunohistochemistry. CircNRIP1 was mainly localized in OS cell cytoplasm and significantly lower in OS cell lines than in normal human osteoblasts. CircNRIP1 overexpression significantly inhibited OS cell proliferation, migration, and invasion *in vitro*. miR-1200 was predicted as the sponge miRNA of circNRIP1 and directly interacted with circNRIP1 confirmed by the dual-luciferase reporter assay. Moreover, miR-1200 overexpression significantly alleviated the inhibitory effect of circNRIP1 on OS cells. A protein-coding gene MIA2 was identified as the miR-1200 targeting gene and reversely associated with miR-1200 expression in OS cells. Increase in MIA2 expression in a murine OS cell xenograft model was associated with circNRIP1 expression in inhibition of OS cell xenograft growth *in vivo*. These data support the circNRIP1 OS-suppressive role by sponge of miR-1200 expression and in turn to upregulate MIA2 expression.

Keywords: Circular RNA, circNRIP1, osteosarcoma, MIA2, miR-1200

Introduction

Osteosarcoma (OS) is the most common malignant bone tumor that arises from mesenchymal cells and mainly occurs in adolescents and children [1]. Approximately 15-20% of patients are diagnosed with metastasized OS at their first visit and the most frequent metastatic site is the lung [2-4]. Despite the advancement in OS diagnosis and treatment, the 5-year OS survival rate is still very low and the recurrence rate is correspondingly high, which may be due to the commonly occurred tumor drug resistance and distant metastasis [4]. Therefore, further research and better understanding of OS pathogenesis could lead to novel therapeutic strategies and biomarker discovery for OS patients.

Towards this end, circRNAs, a class of non-coding RNA that was once considered as error byproducts in the genome, have recently become a hot topic of basic and translational research given their important functions in cancer and embryo development [5]. Genetically, circRNAs are derived from protein-coding genes and/or produced by backward splicing [6-8]. Previous studies have shown that circRNAs reg-

ulate tumor progression in different ways, such as the miRNA "sponge", RNA-pro binding, and protein translation [9-13]. Alteration of circRNA expression and functions was associated with development of various human cancers, like nasopharyngeal carcinoma, breast cancer, and lung cancer [14-17]. Different circRNAs have shown to possess different roles in human tumorigenesis; for example, circLARP4 and hsa-circ-000248 inhibited tumor cell proliferation [18, 19], whereas circ-DONSON and circDLG1 promoted gastric cancer [20, 21]. In this study, we focused on circNRIP1, a circRNA arising from the gene NRIP1, has been shown to influence the progression of many malignancies, including cervical and gastric cancers as well as osteosarcoma [22-24]. However, to date, there are only a few studies of circNRIP1 in human cancers and the role of circNRIP1 in OS progression and mechanism of the action have not been fully elucidated.

Melanoma inhibitory activity 2 (MIA2), mapped to human chromosome 14q13, belongs to the novel MIA gene family, which includes genes MIA, OTOR, and TANGO and shares important structural features [25]. MIA2 has been found to be almost exclusively expressed in hepatocytes but lowly expressed in hepatocellular carcinoma (HCC) [26]. Thus, the role of MIA2 protein could be closely associated with liver injuries or diseases [27]. Decrease in MIA2 expression or MIA2 deficiency significantly correlated with HCC development and that MIA2 expression inhibited HCC cell proliferation, indicating a tumor suppressive activity of MIA2 in HCC [28]. Moreover, MIA2 has been shown to play an oncogenic role in oral squamous cell carcinoma (OSCC), as MIA2 expression was detected in most of the OSCCs and was associated with tumor expansion and nodal metastasis, whereas knockdown of MIA2 expression reduced human tongue squamous carcinoma (HSC3) cells invasion capacity, suggesting that targeting of MIA2 expression could be a potential treatment approach for OSCC [29, 30]. To date, the role of and association between MIA2 and osteosarcoma development is still unknown.

In this study, we detected circNRIP1 expression in OS cell lines vs. normal human osteoblast cells. We investigated and assessed the role of circNRIP1 expression in OS cell proliferation, migration, and invasion *in vitro* and OS cell xenograft formation and growth *in vivo*. After that, we predicted and confirmed the circNRIP1 sponging miR-1200 and its target gene MIA2. We first analyzed the differential expression of MIA2 in OS cell lines. Taken together, we expected to provide novel information regarding circNRIP1 as a tumor suppressor in OS development through the miR-1200-MIA2 axis, which could be used as a novel approach to control OS progression clinically in the future.

Methods

Cell lines and culture

A normal human osteoblast hFOB1.19 cell line and osteosarcoma cell lines MG-63, MNNG/HOS, 143B, and U2OS were originally obtained from Shanghai Cell Collection (Shanghai, China). hFOB1.19 cells were maintained in Dulbecco's modified Eagle's medium (DMEM)/F-12, while MG63 and HOS cells were maintained in DMEM, and U2OS and 143B cells were maintained in McCoy's 5a and Roswell Park Memorial Institute medium-1640 (RPMI-1640). All growth media were supplemented with 10% fetal bovine serum (FBS; Gibco, Gaithersburg, MD, USA) and cultured at either 37°C in 5% CO_2 for OS cell lines or at 33.5°C in 5% CO_2 for hFOB1.19.

RNA in situ hybridization (RNA FISH)

Cy3-labeled circNRIP1 probe and RNA FISH kit were designed by and obtained from Genepharma (Shanghai, China). The sequence of the probe was 5'-TCACAATCCAAACACTTCCGTCTGTCTCCAAGCTCTGA-3'. For the FISH assay, 1×10^4 HOS and U2OS cells were seeded and grown in glass cell culture dishes for 24 h and then fixed with 4% paraformaldehyde and incubated with 1% buffer A to increase cell membrane permeability. After that, cells were incubated overnight with the circNRIP1 probe working solution. After 24 hours, the nuclei were stained with DAPI (4',6-diamidino-2-phenylindole) staining solution for approximately 20 minutes at 24°C. The cells were captured images using the laser confocal system (Leica TCS SP5).

RNA, DNA extraction and qRT-PCR

Total RNA was isolated from cells and OS cell xenografts using TRIzol reagent (Invitrogen, Carlsbad, CA, USA) according to the manufac-

Table 1. Primers used for qRT-PCR analysis

Gene	Primers sequences
circNRIP1	5'-TCAACAGCCTTCTCAATTTTCT-3'
	5'-TCACAATCCAAACACTTCCGT-3'
NRIP1	5'-GGATCAGGTACTGCCGTTGAC-3'
	5'-CTGGACCATTACTTTGACAGGTG-3'
MIA2	5'-GAGGCCCATTCTTGAGAAGAGG-3'
	5'-TTGAAGGTGGAATCAAACCTGAG-3'
GAPDH	5'-CAGGAGGCATTGCTGATGAT-3'
	5'-GAAGGCTGGGGCTCATTT-3'

turer's protocol. The RNA extraction kit (Norgen Biotek, Canada) was used to separate the nuclear and cytoplasmic RNA. In particular, the cells were first lysed using pre-cooled lysate J and then centrifuged, the supernatant contained cytoplasmic RNA while the precipitated pellet was nuclear RNA. Then, the buffer SK was added separately to the tubes, mixed well, and centrifuged to obtain cytoplasmic and nuclear RNA respectively. Purified RNA samples were stored at -20°C for a short period of time or reversely transcribed into cDNA immediately using the PrimerScript regent Kit (TAKARA, Dalian, China). qRT-PCR was performed to quantitate gene expression using an UltraSYBR Mixture kit from CWBIO (Shanghai, China) according to their instructions. The divergent primers for amplification of circNRIP1 were synthesized by Genepharma and primers for amplification of miRNAs were supplied with RiboBio (Guangzhou, China). The relative levels of miRNAs and circRNA/mRNA expression were normalized to the U6 and GAPDH levels, respectively. The relative expression level of each gene was calculated by the $2^{-\Delta\Delta Ct}$ method. The sequence of primers for circRNA and mRNA are listed in **Table 1**.

RNase R treatment

The procedures of extracting total RNA of HOS and MG63 cells were the same as the above. For the RNase R treatment, 2 μg of total RNA was incubated at 37°C for 30 min with or without 3 U/μg RNase R (Epicentre Technologies, Madison, WI, USA). After digestion, the relative level of circNRIP1 expression was detected by using qRT-PCR.

Plasmid construction and cell transfection

Plasmids for overexpressing circNRIP1 were designed and provided by Genepharma, and the vector pcDNA3.1 was used as the negative control. The mimics/inhibitor of miR-1200 and the matched negative control (NC) were from by RiboBio (Guangzhou, China). For cell transfection, cells were inoculated in 6-well plates until reached approximately 50% confluency and then transfected with plasmids using Lipofectamine 3000 (Invitrogen) according to the manufacturer's instructions. The transfection efficiency of plasmids was verified by qRT-PCR.

5-ethynyl-20-deoxyuridine (EdU) assay

The ability of OS cell proliferation was evaluated using the Cell-Light EdU Apollo567 In Vitro Kit (RiboBio). In short, the OS cells were cultured in 96-well plates at 10,000 per well. After diluting at a concentration of 1:1000, 100 μl of buffer A was added into each well and incubated at 37°C for 2 h and cells were fixed with 4% paraformaldehyde for 30 min. Next, the cells were maintained in freshly prepared EdU solution in dark for 40 min, added with 100 μL of Hoechst33342 to each well to visualize the nuclei for 30 min. The proliferation ability of OS cells was evaluated by recording five randomly selected fields under a microscope.

Cell viability CCK-8 assay

The CCK-8 assay was conducted to evaluate cell viability. In brief, cells were seeded into 96-well plates at a density of 6000 cells per well after different treatments. Next, the cell culture medium was refreshed with a medium containing 10% CCK-8 (Dojindo, Ogawamachi Gonoe, Japan) and cells were further cultured for 1 h. At the end of experiment, the optical density (OD) was detected using a microplate reader (Geneomaga) at 450 nm under lightproof conditions.

Wound healing assay

The transfected cells were planted into the 6-well plate and grown to reach approximately 80-85% confluency, and then vertically scratched with a 200 μL pipette. At 0 h and 24 h after scratch, the field of view was randomly selected to take photos of each scratched area using Nikon ECLIPSE (Nikon, Tokyo, Japan). The relative degree of cell migration was calculated after normalizing the reduced distance to the induced damage area and compared to the 0 h control group.

Transwell migration and Matrigel invasion assay

MG63 and U2OS cells were planted into the 24 well chambers containing plates for the Transwell assays. When reached 90% density, the transfected cells were digested with trypsin. Cells were resuspended in 200 μL of serum-free medium and drop-wise added to the upper chamber (2×10^4 cells per well for migration assay, 8×10^4 cells per well for invasion assay), and the medium containing 10% FBS was placed in the lower chamber. The cells were grown for 24 h. The un-migrated cells were gently wiped with sterile cotton swabs, whereas the migrated cells were fixed and then stained with 1% crystal violet for 40 min. The Transwell filters were placed under an inverted microscope and photographed for at least three randomly selected fields for each filter. The filters pre-coated with Matrigel (BD Bioscience, San Jose, CA, USA) were used for the invasion assay.

Colony formation assay

The transfected MG63 and U2OS cells were seeded into 6-well plates at a density of 1000 cells per well and grown for 15 days with medium refresh every three days. At the end of experiment, cells were washed twice with ice-cold phosphate-buffered saline (PBS) and fixed in 1 mL of 4% paraformaldehyde for 30 min and then stained with 1% crystalline violet for 30 min. The cell colony-forming ability was measured by counting cell clones with 50 or more cells.

Predicted miRNA targets of circNRIP1

We analyzed the miRNA binding sites of circNRIP1 in three bioinformatics databases including miRanda (http://www.microrna.org), circinteractome (https://circinteractome.nia.nih.gov/), RNAhybrid (https://bibiserv.cebitec.uni-bielefeld.de/rnahybrid/) [31]. The constraints used for filtering were (a) Total score ≥140 and Total energy <4 kcal/mol; (b) Numbers of predicted binding sites ≥1 and context+ score percentile ≥80; and (c). Numbers of binding position >0.

Predicted target genes of miR-1200

The target genes of miR-1200 were predicted using the Targetscan (http://www.targetscan.org/vert_71/), miR DIP (http://ophid.utoronto.ca/mirDIP/index.jsp), miRWalk (http://mirwalk.umm.uni-heidelberg.de/). The constraints used for filtering were (a) |Total context++ score| >0.35; (b) Minimum score ≥ High; and (c) The binding region length >25 and longest consecutive pairings >10.

Dual-luciferase reporter assay

We used the RNAhybrid analyses to predict the binding sites between circNRIP1 and miR-1200. The circNRIP1 sequence or a mutant sequence and the MIA2 sequence or a mutant sequence were subcloned into the pmirGLO vector (RiboBio), respectively. To validate the targeting relationship, HEK-293T cells and HOS cells were seeded into 24 well plates and grown overnight and then subjected to transfection when cell density reaches 60%. After that, cells were co-transfected with miR-1200 mimics and reporter plasmids and each experiment was in triplicates. At 48 h after transfection, the luciferase activity was evaluated using the Dual Luciferase Reporter Assay System (Promega, Madison, WI, USA). For comparison, the firefly luciferase activity was used to normalize to the Renilla luciferase activity.

A nude mouse OS cell xenograft model

Gem Pharmatech Co., Ltd. (Nanjing, China) provided us with four-week-old male BALB/c nude mice, which were housed in a sterile environment and fed a sterile diet. Cells transiently transfected with plasmids and siRNAs have been used for nude mouse experiments [32, 33]. For the in vivo assay, HOS cells were transfected with circNRIP1 expression plasmids and control plasmids and 5×10^6 treated HOS cells were subcutaneously injected to each mouse into the left abdominal back. The weight of the mice was measured every three days after the HOS cells were inoculated and 4 weeks later, all nude mice were sacrificed and tumor tissues were taken and then weighed and embedded in paraffin and sectioned for H&E staining and immunohistochemistry. Prior approval was obtained from the ethics committee of the host institution prior to conducting the experiments.

Western blot

Cells were lysed using radioimmunoprecipitation assay buffer (RIPA buffer) containing protease inhibitors to obtain total cellular protein.

The equal amount of protein samples were separated in 10% sodium dodecyl sulfate-polyacrylamide gel electrophoresis (SDS-PAGE) gels using the electrophoresis and then transferred onto the PVDF membranes (Bio-Rad, Hercules, CA, USA). The membranes were incubated in the blocking buffer for about 1 h and then with the specific primary antibody against GAPDH (Cat. #D110016; Sangon Biotech, Shanghai, China) or MIA2 (Cat. #ab58973; Abcam, Cambridge, MA, USA) overnight at 4°C. On the next day, the membranes were incubated with a goat anti-rabbit secondary antibody at the room temperature for 1 h. The positive signals corresponding to the protein bands were detected using chemiluminescence Kit (Beyotime, Shanghai, China).

Hematoxylin and eosin staining

The paraffin-embedded OS cell xenograft samples were dewaxed with xylene and rehydrated in a series of ethanol solution and into water. After that, the tissue sections were stained with hematoxylin for 10 min and then treated in solutions of hydrochloric acid in ethanol and ammonium hydroxide for 30 s each and stained with eosin for 1 min. The sections were then placed into bottles filled with gradient concentrations of 70%, 80%, 90%, and 100% ethanol solution for about 15 s each, respectively. Next, the sections were cleared in xylene three times for 3 min each and mounted with the neutral gum (Biosharp, Beijing, China).

Immunohistochemistry (IHC)

The IHC was performed on xenograft mouse tissue sections. In brief, the paraffin-embedded osteosarcoma cell xenografts were sectioned into 5 μm-thick sections and then placed onto a 65°C plate and baked for 1 h. After that, sections were dewaxed in xylene and rehydrated in a series of ethanol solution and into water. Thereafter, 100 μl of 3% hydrogen peroxide solution was added onto each slide for 3 min. After washing in PBS twice, the sections were incubated with 100 μL of a primary antibody at 4°C overnight, and then maintained in 100 μL of the vision biosystems TM (rq7100) at 25°C for 25 min and incubated with 3,3'-diaminobenzidine (DAB) solution briefly and then counterstained with hematoxylin, dehydrated, fixed, and mounted. Finally, the sections were reviewed and photographed under a light microscope (Nikon ECLIPSE).

Microarray data

The data on differentially expressed circRNAs in OS cells were obtained from the NCBI Gene Expression Omnibus (GEO) with the accessing number of GSE96964.

Statistical analysis

All data were obtained from at least three independent replicates. The difference between the two groups was compared using the Student's *t*-test, while the one-way analysis of variance (ANOVA) test was performed for statistical analysis of three groups or more. The GraphPad Prism software version 6.0 was used for all statistical analyses, while a $P<0.05$ was considered to be statistically significant.

Results

Downregulation of circNRIP1 in human OS cell lines

CircNRIP1 has been reported to promote the proliferation of cervical cancer and gastric cancer [22, 24, 34] but less studied in osteosarcoma [23]. In this study, we first downloaded the microarray data on OS from the GEO database (GSE96964) and analyzed the differential expression of all circRNAs [35]. We obtained the TOP 81 circRNAs that were either up-regulated or down-regulated in OS and then generated a heatmap based on their fold change (|fold change| ≥1.5, P<0.05). After eliminating circRNAs that had been deeply studied such as circMYO10 and circTADA2A [36, 37], we selected circNRIP1, which showed the most differential expression in OS cell lines, as our target. As illustrated in **Figure 1A**, level of hsa_circ_0004771 (circNRIP1) expression in OS cells was greatly downregulated compared with the normal bone cell line hFOB1.19. Compared to the h.fob cells, level of circNRIP1 expression was also significantly decreased in OS cell lines (**Figure 1B**). Our results were consistent with the data obtained from microarray data and thus, MG63 and U2OS cells were selected for further investigation for the role and mechanism of circNRIP1 in OS oncogenesis.

Circular structure recognition of circNRIP1 and its cellular localization

Divergent primers and convergent primers were designed for amplification of circNRIP1 and

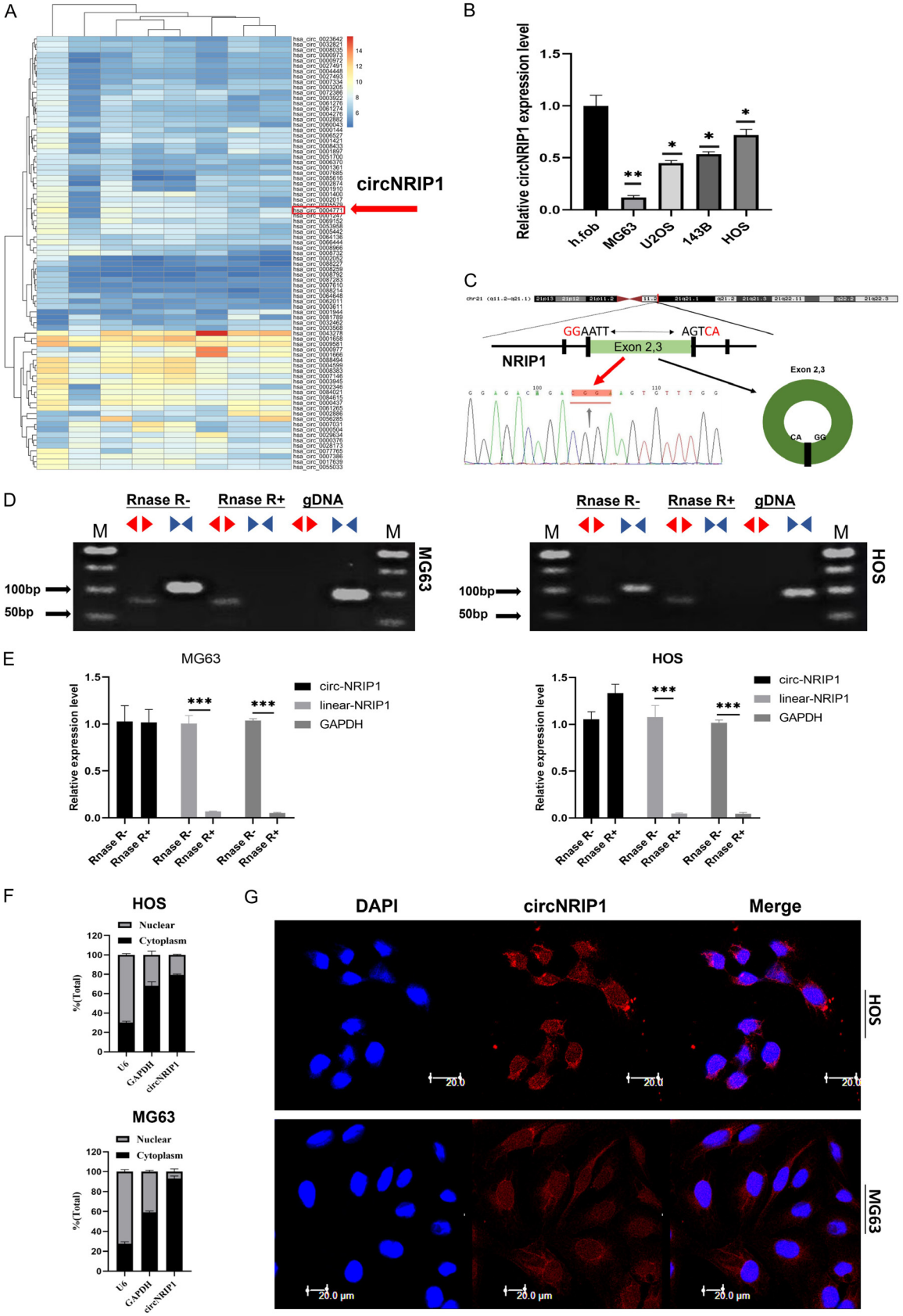
A
circNRIP1
B
Relative circNRIP1 expression level
h.fob
MG63
U2OS
143B
HOS
C
GGAATT
AGTCA
Exon 2,3
NRIP1
D
Rnase R-
Rnase R+
gDNA
M
100bp
50bp
MG63
HOS
E
MG63
HOS
Relative expression level
circ-NRIP1
linear-NRIP1
GAPDH
F
HOS
MG63
Nuclear
Cytoplasm
%(Total)
U6
GAPDH
circNRIP1
G
DAPI
circNRIP1
Merge
HOS
MG63
20.0 μm

Figure 1. Downregulation of circNRIP1 expression in human OS cell lines. A. The heatmap of 17 upregulated and 64 downregulated circRNAs and circNRIP1 is downregulated by 2.86 folds in OS cells. B. qRT-PCR. The data showed that circNRIP1 was downregulated in OS cell lines compared to normal hFOB1.19 cells. All data were normalized to GAPDH levels and demonstrated as $2^{-\Delta\Delta Ct}$. C. The head-to-tail splicing of circNRIP1 was detected by using qRT-PCR and verified by Sanger sequencing. The arrows point the head-to-tail splicing of circNRIP1. D. Agarose gel electrophoresis. We examined circNRIP1 and linear NRIP1 expression levels in OS cells using an agarose gel electrophoresis in the presence or absence of RNase R. The red and blue triangles represent divergent primers and convergent primers respectively. E. qRT-PCR. The data showed that the back-spliced NRIP1 was more stable than the linear forms of NRIP1 in MG63 and HOS cells. F. qRT-PCR. The nuclear RNA and cytoplasmic RNA of MG63 and HOS were extracted respectively and conducted by using qRT-PCR. The results manifested that circNRIP1 expression was mainly occurred in the cytoplasm of OS cells. G. FISH. The results showed that circNRIP1 was mainly present in the cytoplasm (The scale bar, 20 μm). The nucleus was stained by DAPI and circNRIP1 probe was labeled by cy3. $^{***}P<0.001$, $^{**}P<0.01$, and $^{*}P<0.05$.

canonical forms of NRIP1, respectively. To rule out genomic rearrangement and trans-splicing, the products amplified by the divergent primers were analyzed by using the Sanger sequencing and confirmed that circNRIP1 was back-spliced from the head to the tail of the exon 2 and 3 of the NRIP1 gene (**Figure 1C**). After that, we performed an agarose gel electrophoresis assay with cDNA and gDNA from OS cells and found that circNRIP1 was detected in cDNA, but no amplification product was detected in gDNA, further supporting the back-splicing of circNRIP1 in OS cells (**Figure 1D**). To determine the stability of circRNAs and mRNAs, we assessed level of circNRIP1 and linear NRIP1 expression with or without RNase R treatment with qRT-PCR. We found that circNRIP1 was virtually resistant to RNase R digestion, whereas NRIP1 mRNA level was decreased sharply under the RNase R treatment (**Figure 1E**). To confirm the localization of circNRIP1 in OS cells, we performed qRT-PCR and RNA FISH experiments and found that circNRIP1 was predominantly localized in the cytoplasm of OS cells (**Figure 1F**, **1G**).

Inhibition of OS cell migration, invasion and proliferation after circNRIP1 overexpression

To assess the *in vitro* functions of circNRIP1 in OS cells, we transfected the circNRIP1 expression plasmids or a blank vector as a control into MG63 and U2OS cells. The data showed that circNRIP1 was successfully overexpressed in OS cells, while there was no significant change in NRIP1 mRNA expression (**Figure 2A**). The OS cell CCK-8, EdU, and colony formation assays altogether indicated that the OS cell proliferation capacity was reduced significantly after circNRIP1 overexpression (**Figure 2B-D**). The Transwell assay revealed that the upregulation of circNRIP1 inhibited capacity of MG63 and U2OS cell migration and invasion (**Figure 2E**). Overexpression of circNRIP1 also slowed healing of abrasions, showing that OS cell migration was suppressed by wound healing assay (**Figure 2F**). Taken altogether, circNRIP1 impelled a potent tumor suppressor effect on OS cell proliferation, migration and invasion *in vitro*.

CircNRIP1 as a sponge for miR-1200 in OS cells

CircRNAs are well documented to play a miRNA sponge role in cancer cells so as to influence tumor development [38-40]. To identify the potential sponging miRNA of circNRIP1 in OS cells, we conducted bioinformatical analysis using the web-based miRanda, RNAhybrid and circinteractome tools and obtained six candidate miRNAs (**Figure 3A**). We then performed the qRT-PCR analysis and revealed that only hsa-miR-1200 was dramatically decreased in cells overexpressed circNRIP1 among these six candidate miRNAs (**Figure 3B**). Notably, we detected the markedly downregulated miR-1200 expression in HOS and 143B cells but significantly upregulated in MG63 and U2OS cells compared to hFOB1.19 (**Figure 3C**). To determine whether circNRIP1 directly sponges miR-1200 based on their complementary sequence, we performed the bioinformatics analysis using the miRANDA tool and revealed that circNRIP1 shared only one response element with miR-1200 (**Figure 3D**). We then mutated and cloned this responsive element into a luciferase reporter containing the 3'-untranslated region (3'-UTR) of circNRIP1 and co-transfected it with miR-1200 mimics or NC controls into HEK-293 cells and HOS cells. As illustrated in **Figure 3E**, the luciferase activity of the wild-type (WT) reporter in miR-1200 mimics transfected cells was significantly lower than those transfected with miR-1200 mimics NC, while the reporter

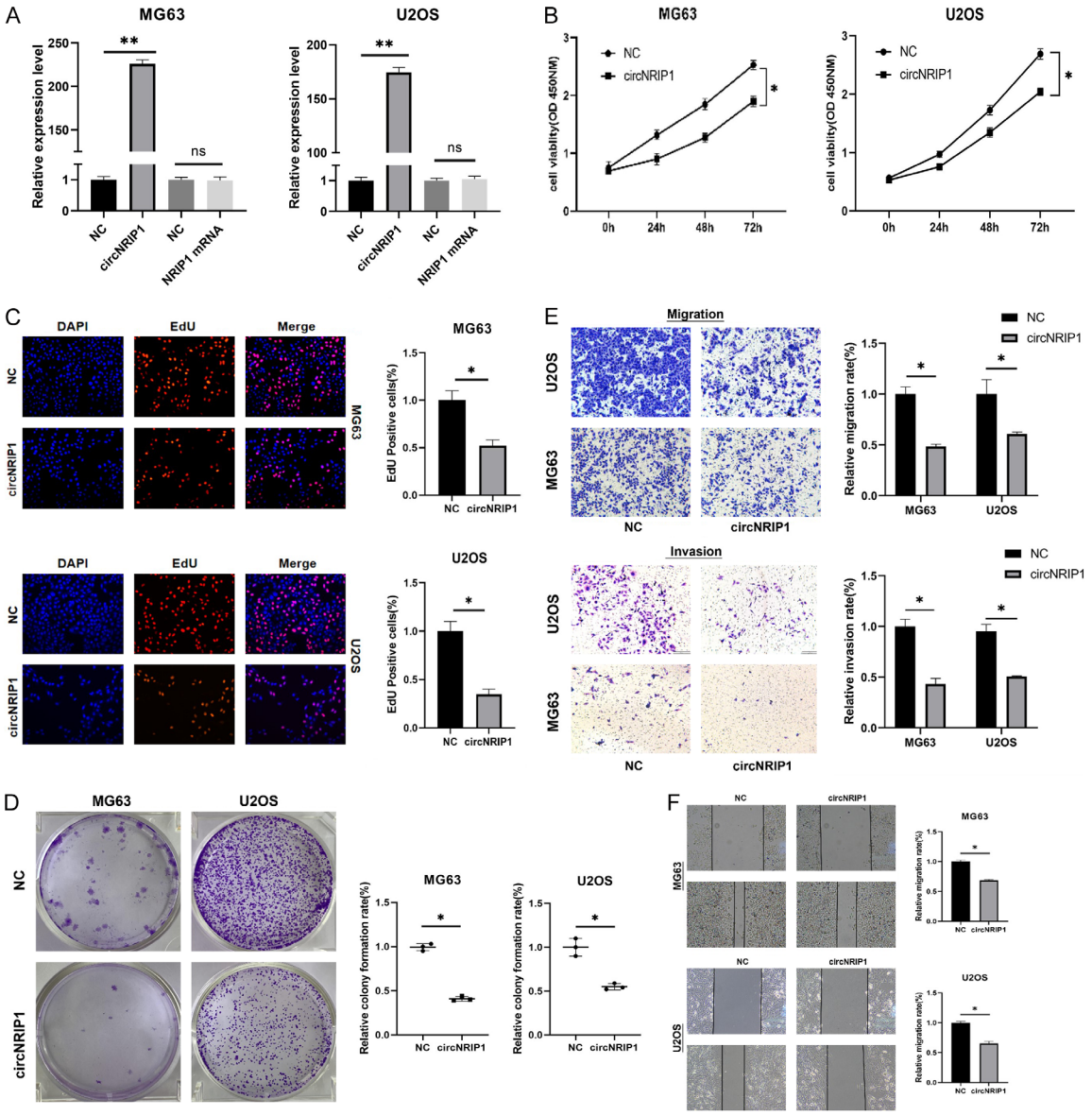

Figure 2. Inhibition of OS cell migration, invasion, and proliferation after circNRIP1 overexpression. A. qRT-PCR. The data verified that circNRIP1 was successfully overexpressed in MG63 and U2OS cells. B. The CCK-8 assay. The data showed that the proliferation ability decreased significantly in OS cells overexpressed circNRIP1. C. EdU assay. The results showed that circNRIP1 overexpression reduced MG63 and U2OS cell proliferation ability. D. Colony formation assay. The experiments showed that circNRIP1 overexpression reduced U2OS and MG63 cell clonogenicity. E. Transwell assay. The data demonstrated that MG63 and U2OS cell migration and invasion rates were reduced after circNRIP1 overexpression. F. Wound healing assay. The data demonstrated that MG63 and U2OS cell migration rate was undermined following circNRIP1 overexpression. $^{**}P<0.01$ and $^{*}P<0.05$.

that contains mutated binding sites has not much changes for the luciferase activity whether the cells were transfected with miR-1200 mimics or NC controls.

To further validate whether circNRIP1 inhibits the proliferation of OS cells by directly interacting with miR-1200, we performed the rescue experiments. Using the CCK-8 (**Figure 3F**), colony formation (**Figure 3G**) and EdU assays (**Figure 3H**), we found that the decreased ability of OS cell proliferation due to overexpression of circNRIP1 was partially restored after co-transfection with miR-1200 mimics. Accordingly, the results of the wound healing (**Figure 4A**) and Transwell assays (**Figure 4B**, **4C**) conveyed that

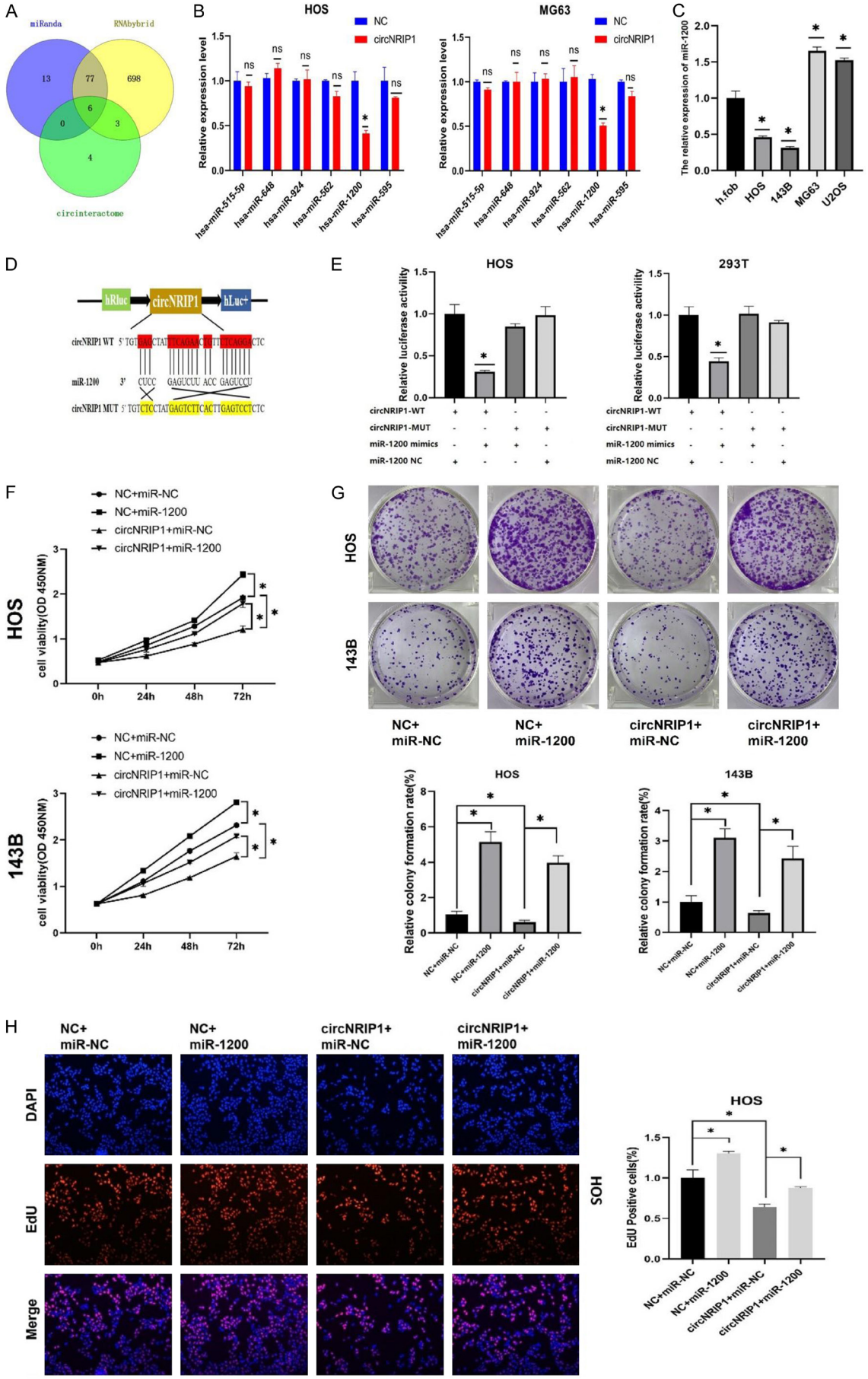
A
miRanda
RNAbybrid
circinteractome
B
HOS
MG63
NC
circNRIP1
Relative expression level
hsa-miR-515-5p
hsa-miR-648
hsa-miR-924
hsa-miR-562
hsa-miR-1200
hsa-miR-595
C
The relative expression of miR-1200
h.fob
HOS
143B
MG63
U2OS
D
hRluc
circNRIP1
hLuc+
circNRIP1 WT
miR-1200
circNRIP1 MUT
E
HOS
293T
Relative luciferase activity
circNRIP1-WT
circNRIP1-MUT
miR-1200 mimics
miR-1200 NC
F
NC+miR-NC
NC+miR-1200
circNRIP1+miR-NC
circNRIP1+miR-1200
HOS
143B
cell viability(OD 450NM)
0h
24h
48h
72h
G
HOS
143B
NC+ miR-NC
NC+ miR-1200
circNRIP1+ miR-NC
circNRIP1+ miR-1200
Relative colony formation rate(%)
H
DAPI
EdU
Merge
SOH
EdU Positive cells(%)

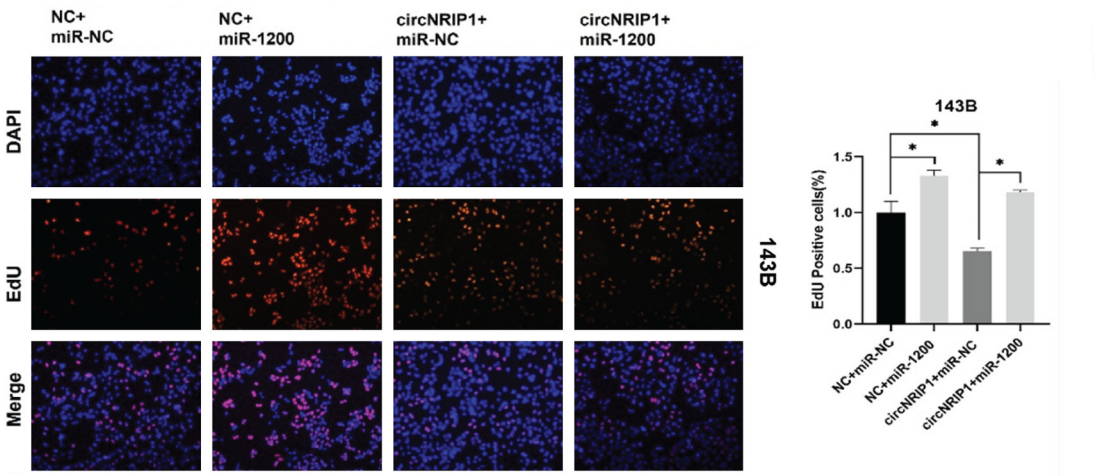

Figure 3. CircNRIP1 as a sponge for miR-1200 in OS cells. A. Bioinformatical analysis. The six target miRNAs of circNRIP1 were predicted by using the online miRanda, RNAhybrid, and circinteractome tools. B. qRT-PCR. The results indicated that only miR-1200 was significantly downregulated in OS cells after overexpressing circNRIP1. C. qRT-PCR. The experiments examined the difference in miR-1200 expression levels in OS cells compared with normal h.fob cells. D. Bioinformatical analysis. CircNRIP1 was predicted to contain a putative binding site of miR-1200. E. Dual-luciferase reporter assay. HEK293T and HOS cells were transfected with miR-1200 mimics and luciferase reporter plasmids containing either a wild type or a mutant circNRIP1 3'-UTR where the binding site of miR-1200 was mutated. The binding site between miR-1200 and circNRIP1 was confirmed in dual-luciferase reporter assay. F and G. CCK-8 and colony formation assay. The data displayed the reduced proliferation ability of HOS and 143B cells after overexpressing circNRIP1 but was ameliorated by miR-1200 overexpression. H. The EdU assay. The data showed that OS cell proliferation rate after over expressing circNRIP1 was partially neutralized by the co-transfection with miR-1200. $^{**}P<0.01$ and $^{*}P<0.05$.

the reduced OS cell migration and invasion induced by circNRIP1 overexpression was partially abrogated by the co-transfection of miR-1200 mimics. Together, these data suggested that circNRIP1 inhibits cell migration, invasion and proliferation by sponging miR-1200.

MiR-1200 targeting MIA2 in OS cells

It is widely accepted that miRNAs regulate tumor growth by inhibiting the expression of their target genes. In order to identify the target genes that miR-1200 might directly bind to in OS cells, we performed the bioinformatical analysis and found 22 candidate target genes (**Figure 5A**). We then performed qRT-PCR analysis in 143B and HOS OS cell lines transfected with miR-1200 mimics and found that only MIA2 was significantly decreased in both OS cell lines (**Figure 5B**). We then, detected level of MIA2 expression in all four OS cell lines *vs.* normal bone cell line hFOB1.19 using qRT-PCR and Western blot. Interestingly, MIA2 was significantly upregulated in 143B and HOS cells but downregulated in MG63 and U2OS cells (**Figure 5C**). After that, we transfected HOS and 143B OS cell lines with miR-1200 mimics and inhibitor respectively, and the results showed that miR-1200 was significantly up- or downregulated in OS cells (**Figure 5D**). The results of qRT-PCR and Western blot assays demonstrated that miR-1200 mimics downregulated level of MIA2 expression, while miR-1200 inhibitor led to upregulated MIA2 expression in both HOS and 143B OS cell lines, respectively (**Figure 5E**). Based on the predicted results of Targetscan, the MIA2 3'-UTR mRNA contained sequences complementary to the miR-1200 seed sequence (**Figure 5F**). To verify whether the gene MIA2 directly binds to miR-1200, we constructed a 3'-UTR sensor and co-transfected OS cells and 293T cells with miR-1200 mimics. We found a decrease in the luciferase activity in cells with miR-1200. To further confirm the specificity of binding site, we removed all binding sites of miR-1200. The results showed that co-transfection of miR-1200 with the mutant construct abrogated the decreased luciferase activity with wild-type 3'-UTR, indicating that miR-1200 specifically regulates MIA2 expression (**Figure 5G**). Thus, circNRIP1 may function in OS cells to sponge miR-1200 and we next investigated whether circNRIP1 regulates the expression of MIA2. The results showed that level of MIA2 expression was increased in circNRIP1 overexpressed cells

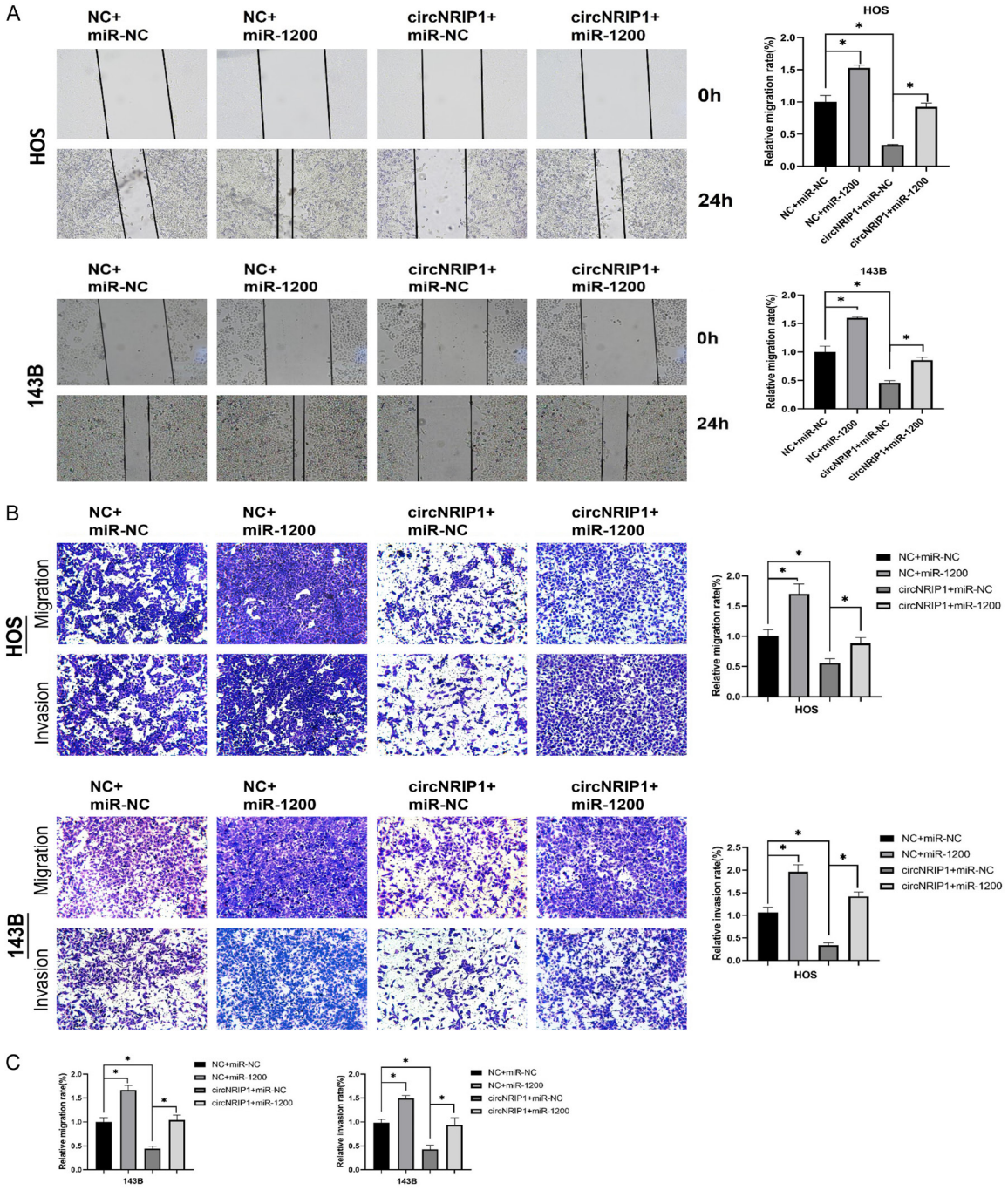

Figure 4. Reversal of circNRIP1 antitumor effects on OS cells after miR-1200 overexpression. A. Wound healing assay. The data showed that HOS and 143B cell migration ability was impeded by circNRIP1 overexpression, which was partially restored by miR-1200 overexpression. B and C. Transwell assay. The data demonstrated decrease in OS cell migration and invasion rates after circNRIP1 overexpression was partially rescued by the co-transfection with miR-1200 mimics. $^{**}P<0.01$ and $^{*}P<0.05$.

(**Figure 5H**). Similarly, levels of MIA2 mRNA and protein were increased to a greater extent in cells overexpressing circNRIP1 alone than in cells co-transfected with circNRIP1 and miR-1200 mimics (**Figure 5I**).

CircNRIP1 inhibition of OS cell xenograft growth in vivo

To investigate the *in vivo* function of circNRIP1 in OS cell xenograft growth, we established and

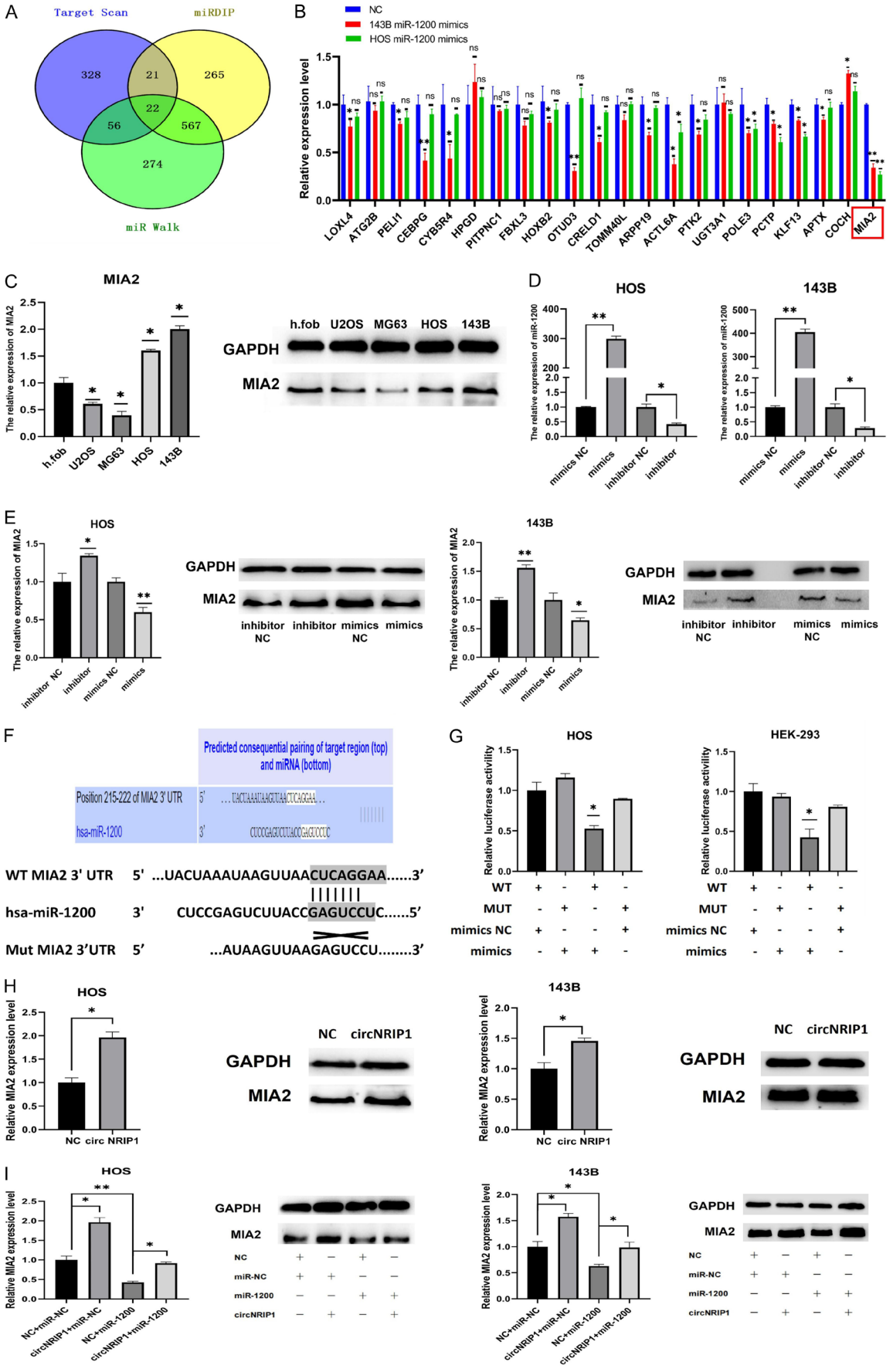
A
Target Scan
miRDIP
miR Walk
328
21
265
22
56
567
274
B
NC
143B miR-1200 mimics
HOS miR-1200 mimics
Relative expression level
LOXL4
ATG2B
PELI1
CEBPG
CYB5R4
HPGD
PITPNC1
FBXL3
HOXB2
OTUD3
CRELD1
TOMM40L
ARPP19
ACTL6A
PTK2
UGT3A1
POLE3
PCTP
KLF13
APTX
COCH
MIA2
C
MIA2
The relative expression of MIA2
h.fob
U2OS
MG63
HOS
143B
GAPDH
MIA2
D
HOS
143B
The relative expression of miR-1200
mimics NC
mimics
inhibitor NC
inhibitor
E
HOS
143B
The relative expression of MIA2
inhibitor NC
inhibitor
mimics NC
mimics
GAPDH
MIA2
F
Predicted consequential pairing of target region (top) and miRNA (bottom)
Position 215-222 of MIA2 3' UTR
hsa-miR-1200
WT MIA2 3' UTR 5' ...UACUAAAUAAGUUAACUCAGGAA.....3'
hsa-miR-1200 3' CUCCGAGUCUUACCGAGUCCUC.....5'
Mut MIA2 3'UTR 5' ...AUAAGUUAAGAGUCCU.....3'
G
HOS
HEK-293
Relative luciferase activity
WT
MUT
mimics NC
mimics
H
HOS
143B
Relative MIA2 expression level
NC circ NRIP1
NC
circNRIP1
GAPDH
MIA2
I
HOS
143B
Relative MIA2 expression level
NC+miR-NC
circNRIP1+miR-NC
NC+miR-1200
circNRIP1+miR-1200
GAPDH
MIA2
NC
miR-NC
miR-1200
circNRIP1

Figure 5. miR-1200-targeting of MIA2 expression in OS cells. A. Bioinformatical analysis. The targeting genes of miR-1200 were predicted by using the online Target Scan, miRDIP, and miR Walk tools and there were 22 candidate genes, including MIA2, identified thereafter. B. qRT-PCR. Among the 22 candidate target genes examined, only MIA2 was significantly decreased in both 143B and HOS cells. C. qRT-PCR and Western blot. MIA2 was differentially expressed in OS cell lines and h.fob cells as demonstrated by qRT-PCR and Western blot. D. qRT-PCR. miR-1200 mimics upregulates miR-1200 effectively, whereas its inhibitor significantly downregulates miR-1200 in HOS and 143B cells. E. qRT-PCR and Western blot. The data confirmed that miR-1200 overexpression was able to significantly inhibit MIA2 expression in OS cells, whereas knockdown of miR-1200 expression increased level of MIA2 expression. F. Targetscan analysis. The data illustrated that the possible binding sites of miR-1200 to *MIA2* predicted by the Targetscan with wild type or mutant MIA2 3'-UTR. G. Dual-luciferase reporter assay. The interaction between miR-1200 and the putative binding sites was confirmed by a dual-luciferase reporter assay. H. qRT-PCR and Western blot. The positive correlation between circNRIP1 and MIA2 gene was verified and demonstrated by using qRT-PCR and western blot data. I. qRT-PCR and Western blot. The assays indicated that miR-1200 overexpression decreased MIA2 level and was attenuated by circNRIP1 co-transfection. $^{**}P<0.01$ and $^{*}P<0.05$.

evaluated a OS cell xenograft model in nude mice. HOS cells or HOS cells transiently overexpressed circNRIP1 were subcutaneously injected into nude mice, the weight of tumor tissue was recorded every three days after a week of cell injection, and the results showed that circNRIP1 was able to significantly restrain the size and weight of OS cell xenografts (**Figure 6A-C**). Our qRT-PCR analysis showed that compared with the NC group, level of circNRIP1 expression was significantly higher while the miR-1200 expression levels were significantly lower in the circNRIP1 overexpression group (n=3 each group of mice; **Figure 6D**). H&E staining of mouse OS cell xenograft sections showed significant difference in tumor histomorphology between groups (**Figure 6E**). Abnormalities, such as larger nuclei, deeper staining, and multiple nucleoli were observed in OS cell xenograft tissues of the NC group rather than in the circNRIP1 overexpression group. We have also performed IHC assay on sections of the xenografted tumor tissues, and increase in MIA2 expression was observed in tissues from mice overexpressed circNRIP1 (**Figure 6F**). Thus, circNRIP1 exerts its inhibitory effect on OS progression through the miR-1200/MIA2 axis *in vivo*.

Discussion

The 5-year osteosarcoma survival rate, especially for metastasized OS, is very low [41]. Therefore, better understanding of the pathological mechanisms and identification of novel molecular targets are surely important to develop novel OS therapeutics or early detection biomarkers. circRNAs, a class of single-stranded RNA, form a covalently closed continuous loop, which is different from linear RNA, and play a crucial role in development and progression of various human cancers and could be important biomarkers for tumor early detection [42] because circRNAs have been shown to play a regulatory role in both physiological and pathological phases of diseases or embryo development [43-45]. For instance, ciRS-7 is a circRNA derived from the parental gene CDR1 and was one of the first circRNAs that has been shown to sponge miR-7 and caused reduced miR-7 expression in development of colorectal and colon cancer [46, 47]. As to circNRIP1, it has been reported that circNRIP1 was highly expressed in OS cells and promoted OS cell proliferation and migration by sponging miR-199a expression and in turn upregulating expression of the oncogenic gene FOXC2 *in vitro* [23]. In our current study, circNRIP1 was shown to be downregulated in OS cells after bioinformatic analysis and our further qRT-PCR experiments. Moreover, the significant tumor suppressive effect of circNRIP1 was demonstrated in both OS cell lines and nude mouse OS cell xenograft model. As we know, circRNAs usually function by sponging miRNAs and their target genes [48, 49]. Our current study identified miR-1200 as the possible sponge miRNA of circNRIP1 and confirmed the bioinformatical data using the dual-luciferase reporter assay for the direct interaction between miR-1200 and circNRIP1. More importantly, we found that circNRIP1 inhibition of OS cell proliferation, migration and invasion was associated with circNRIP1 downregulation in OS cells; however, overexpression of miR-1200 significantly alleviated the inhibitory effect of circNRIP1 on OS cells, further supporting miR-1200 as the sponging miRNA of circNRIP1.

To further explore the mechanism of miR-1200 in OS cells, we performed bioinformatics analysis and revealed that the tumor suppressor

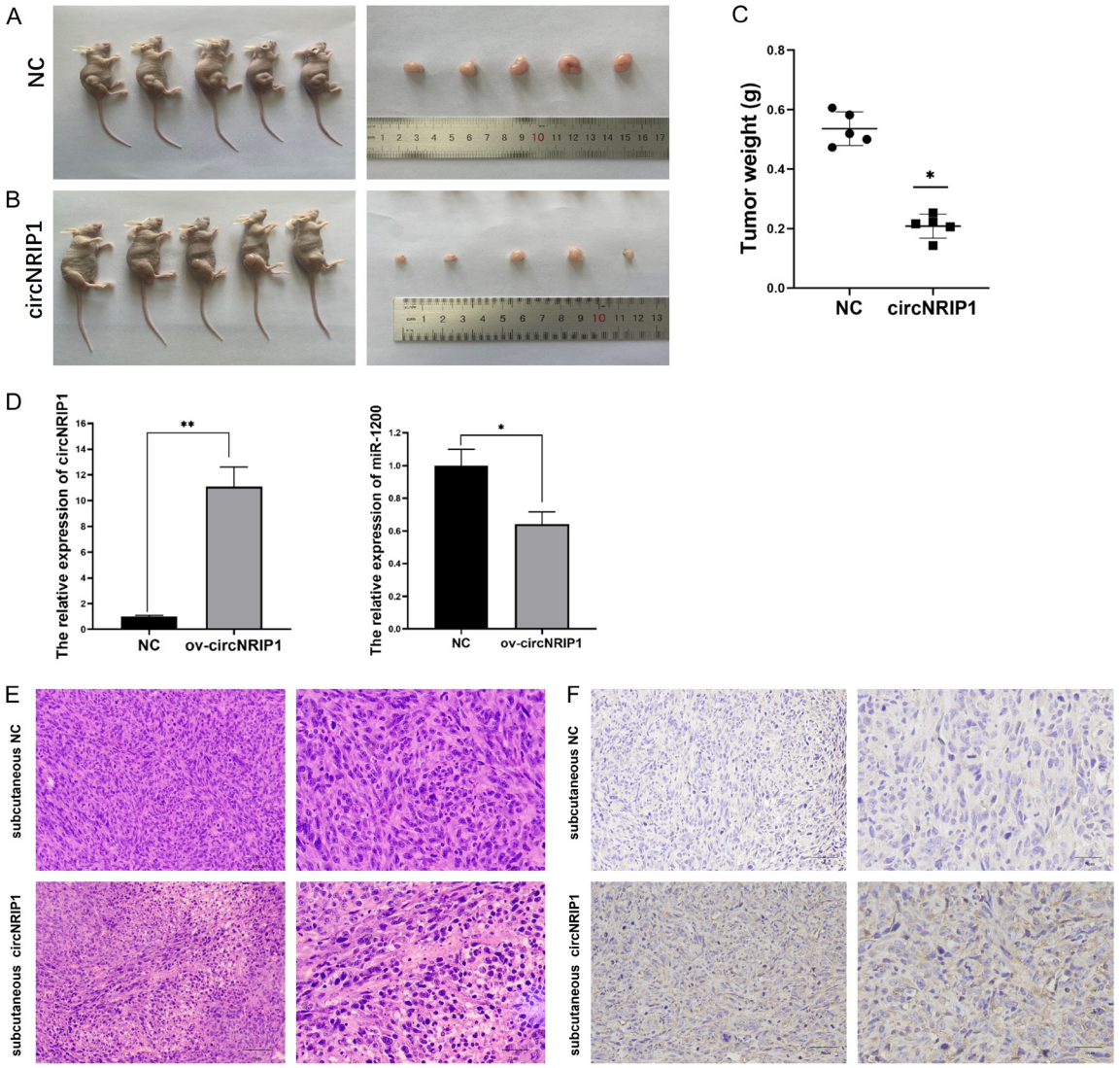

Figure 6. CircNRIP1 inhibition of nude mouse OS cell xenograft formation and growth *in vivo*. A and B. Macro pathology. After subcutaneous injection of HOS cells into nude mice to form tumors (5 per group), tumor volume was significantly smaller in the group of circNRIP1 overexpressed OS cells in mice compared to the negative control group (NC). C. The tumor weights in mice of the circNRIP1 overexpression group were less heavy compared to the NC group. D. Expression levels of circNRIP1 and miR-1200 were measured by using qRT-PCR (n=3). E. H&E staining. The data showed distinct morphological features in the circNRIP1-overexpressed group compared with the NC group (the left, ×200; the right, ×400). F. IHC. The assay was performed and showed that increased expression of MIA2 was observed in tissues from mice overexpressed circNRIP1 (the left, ×200; the right, ×400). $^{**}P<0.01$ and $^{*}P<0.05$.

gene MIA2 may be a targeting gene of miR-1200. It has been reported by multiple studies that MIA2 is significantly reduced in a variety of malignancies, including hepatocellular carcinoma, gastric cancer, and acute lymphoblastic leukemia, and that loss of MIA2 has been frequently associated with advanced tumor stages, indicating its tumor suppressive role [28, 50, 51]. In our research, we detected decreased MIA2 expression in OS cell lines and our nude mouse OS cell xenograft model also revealed a positive correlation between the proliferation of osteosarcoma and the lower expression of MIA2. Our data also showed that miR-1200 significantly inhibited level of MIA2 expression in OS cells. To the best of our knowledge, we have for the first time reported the association between MIA2 expression with osteosarcoma

progression and that circNRIP1 may play its function in OS development via the miR-1200/MIA2 axis.

Interestingly, we notice that circNRIP1 actually induced a stronger effect than miR-1200, indicating there might be additional mechanisms occurred in OS cells, other than only the circNRIP1/miR-1200/MIA2 axis, for the role of circNRIP1 in OS, which needs further investigation. However, our current study is among a few to first discover the role of circNRIP1 in OS cells, which indeed is preliminary because all of experiments were in vitro and in vivo, but there was no ex vivo data to support; thus, further studies are needed to reveal how circNRIP1 is regulated in OS cells and what circNRIP1-related signaling in OS development and progression.

Conclusions

In summary, we have demonstrated that circNRIP1 was downregulated in OS cell lines. CircNRIP1 expression was able to significantly inhibit OS cell proliferation, migration, and invasion *in vitro* and *in vivo*. Mechanistically, circNRIP1 acts as a miRNA sponge by interaction with miR-1200 and its target gene MIA2, leading to the upregulation of MIA2 expression and eventually inhibition of osteosarcoma progression.

Acknowledgements

This study was supported in part by grants from the Jiangsu provincial key research and development program (#BE2020679 to Q.Z.).

Disclosure of conflict of interest

None.

Address correspondence to: Dr. Qiping Zheng, Department of Hematological Laboratory Science, Jiangsu Key Laboratory of Medical Science and Laboratory Medicine, School of Medicine, Jiangsu University, Zhenjiang 212013, Jiangsu, China; Shenzhen Walgenron Bio-Pharm Co., Ltd., Shenzhen 518118, Guangdong, China. E-mail: qp_zheng@hotmail.com

References

[1] Geller DS and Gorlick R. Osteosarcoma: a review of diagnosis, management, and treatment strategies. Clin Adv Hematol Oncol 2010; 8: 705-718.

[2] Gelderblom H, Jinks RC, Sydes M, Bramwell VH, van Glabbeke M, Grimer RJ, Hogendoorn PC, McTiernan A, Lewis IJ, Nooij MA, Taminiau AH and Whelan J; European Osteosarcoma Intergroup. Survival after recurrent osteosarcoma: data from 3 European osteosarcoma intergroup (EOI) randomized controlled trials. Eur J Cancer 2011; 47: 895-902.

[3] Bielack SS, Kempf-Bielack B, Delling G, Exner GU, Flege S, Helmke K, Kotz R, Salzer-Kuntschik M, Werner M, Winkelmann W, Zoubek A, Jurgens H and Winkler K. Prognostic factors in high-grade osteosarcoma of the extremities or trunk: an analysis of 1,702 patients treated on neoadjuvant cooperative osteosarcoma study group protocols. J Clin Oncol 2002; 20: 776-790.

[4] Whelan JS and Davis LE. Osteosarcoma, chondrosarcoma, and chordoma. J Clin Oncol 2018; 36: 188-193.

[5] Sanger HL, Klotz G, Riesner D, Gross HJ and Kleinschmidt AK. Viroids are single-stranded covalently closed circular RNA molecules existing as highly base-paired rod-like structures. Proc Natl Acad Sci U S A 1976; 73: 3852-3856.

[6] Jeck WR and Sharpless NE. Detecting and characterizing circular RNAs. Nat Biotechnol 2014; 32: 453-461.

[7] Kristensen LS, Andersen MS, Stagsted LVW, Ebbesen KK, Hansen TB and Kjems J. The biogenesis, biology and characterization of circular RNAs. Nat Rev Genet 2019; 20: 675-691.

[8] Memczak S, Jens M, Elefsinioti A, Torti F, Krueger J, Rybak A, Maier L, Mackowiak SD, Gregersen LH, Munschauer M, Loewer A, Ziebold U, Landthaler M, Kocks C, le Noble F and Rajewsky N. Circular RNAs are a large class of animal RNAs with regulatory potency. Nature 2013; 495: 333-338.

[9] Zhang ML, Huang NN, Yang XS, Luo JY, Yan S, Xiao FZ, Chen WP, Gao XY, Zhao K, Zhou HK, Li ZQ, Ming L, Xie B and Zhang N. A novel protein encoded by the circular form of the SHPRH gene suppresses glioma tumorigenesis. Oncogene 2018; 37: 1805-1814.

[10] Tay Y, Rinn J and Pandolfi PP. The multilayered complexity of ceRNA crosstalk and competition. Nature 2014; 505: 344-352.

[11] Zheng FX, Wang M, Li YW, Huang C, Tao D, Xie F, Zhang H, Sun JY, Zhang CH, Gu CH, Wang ZD and Jiang GS. CircNR3C1 inhibits proliferation of bladder cancer cells by sponging miR-27a-3p and downregulating cyclin D1 expression. Cancer Lett 2019; 460: 139-151.

[12] Stagsted LVW, O'Leary ET, Ebbesen KK and Hansen TB. The RNA-binding protein SFPQ preserves long-intron splicing and regulates cir-

cRNA biogenesis in mammals. Elife 2021; 10: e63088.
[13] Panda AC. Circular RNAs act as miRNA sponges. Adv Exp Med Biol 2018; 1087: 67-79.
[14] Chen B, Wei WD, Huang XJ, Xie XH, Kong YN, Dai DN, Yang L, Wang J, Tang HL and Xie XM. circEPSTI1 as a prognostic marker and mediator of triple-negative breast cancer progression. Theranostics 2018; 8: 4003-4015.
[15] Chen LJ, Nan A, Zhang N, Jia YY, Li X, Ling YH, Dai JB, Zhang SZ, Yang QY, Yi YN and Jiang YG. Circular RNA 100146 functions as an oncogene through direct binding to miR-361-3p and miR-615-5p in non-small cell lung cancer. Mol Cancer 2019; 18: 13.
[16] Hong XH, Liu N, Liang YL, He QM, Yang XJ, Lei Y, Zhang PP, Zhao Y, He SW, Wang YQ, Li JY, Li Q, Ma J and Li YQ. Circular RNA CRIM1 functions as a ceRNA to promote nasopharyngeal carcinoma metastasis and docetaxel chemoresistance through upregulating FOXQ1. Mol Cancer 2020; 19: 33.
[17] Wei HJ, Liu DS, Sun J, Mao Y, Zhao LH, Zhu WB, Xu GY and Gao ZY. Circular RNA circ_0008450 upregulates CXCL9 expression by targeting miR-577 to regulate cell proliferation and invasion in nasopharyngeal carcinoma. Exp Mol Pathol 2019; 110: 104288.
[18] Pan JY, Bao XL and Zhu K. Circular RNA_LARP4 inhibits cell proliferation and invasion of nasopharyngeal carcinoma by repressing ROCK1. Eur Rev Med Pharmacol Sci 2020; 24: 12624.
[19] Li XP, Yang B, Ren HX, Xiao T, Zhang L, Li L, Li MJ, Wang XH, Zhou HG and Zhang WD. Hsa_circ_0002483 inhibited the progression and enhanced the Taxol sensitivity of non-small cell lung cancer by targeting miR-182-5p. Cell Death Dis 2019; 10: 953.
[20] Ding LX, Zhao YY, Dang SW, Wang Y, Li XL, Yu XT, Li ZS, Wei JF, Liu M and Li GD. Circular RNA circ-DONSON facilitates gastric cancer growth and invasion via NURF complex dependent activation of transcription factor SOX4. Mol Cancer 2019; 18: 45.
[21] Chen DL, Sheng H, Zhang DS, Jin Y, Zhao BT, Chen N, Song K and Xu RH. The circular RNA circDLG1 promotes gastric cancer progression and anti-PD-1 resistance through the regulation of CXCL12 by sponging miR-141-3p. Mol Cancer 2021; 20: 166.
[22] Zhang X, Wang S, Wang HX, Cao J, Huang XX, Chen Z, Xu PH, Sun GL, Xu JH, Lv JH and Xu ZK. Circular RNA circNRIP1 acts as a microRNA-149-5p sponge to promote gastric cancer progression via the AKT1/mTOR pathway. Mol Cancer 2019; 18: 20.
[23] Meng YB, Hao DJ, Huang YF, Jia SJ, Zhang JN, He XR, Liu DY and Sun L. Circular RNA circNRIP1 plays oncogenic roles in the progression of osteosarcoma. Mamm Genome 2021; 32: 448-456.
[24] Li XH, Ma NY, Zhang Y, Wei H, Zhang HJ, Pang XA, Li X, Wu D, Wang D, Yang Z and Zhang SL. Circular RNA circNRIP1 promotes migration and invasion in cervical cancer by sponging miR-629-3p and regulating the PTP4A1/ERK1/2 pathway. Cell Death Dis 2020; 11: 399.
[25] Bosserhoff AK and Buettner R. Expression, function and clinical relevance of MIA (melanoma inhibitory activity). Histol Histopathol 2002; 17: 289-300.
[26] Hellerbrand C, Bataille F, Schlegel J, Hartmann A, Muhlbauer M, Scholmerich J, Buttner R, Hofstadter F and Bosserhoff AK. In situ expression patterns of melanoma inhibitory activity 2 in healthy and diseased livers. Liver Int 2005; 25: 357-366.
[27] Bosserhoff AK, Moser M, Scholmerich J, Buettner R and Hellerbrand C. Specific expression and regulation of the new melanoma inhibitory activity-related gene MIA2 in hepatocytes. J Biol Chem 2003; 278: 15225-15231.
[28] Hellerbrand C, Amann T, Schlegel J, Wild P, Bataille F, Spruss T, Hartmann A and Bosserhoff AK. The novel gene MIA2 acts as a tumour suppressor in hepatocellular carcinoma. Gut 2008; 57: 243-251.
[29] Kurihara M, Kirita T, Sasahira T, Ohmori H, Matsushima S, Yamamoto K, Bosserhoff AK and Kuniyasu H. Protumoral roles of melanoma inhibitory activity 2 in oral squamous cell carcinoma. Br J Cancer 2013; 108: 1460-1469.
[30] Kawai R, Sugita Y, Suzumura T, Hattori T, Yoshida W, Kubo K and Maeda H. Melanoma inhibitory activity and melanoma inhibitory activity 2 as novel immunohistochemical markers of oral epithelial dysplasia. J Clin Med 2021; 10: 3661.
[31] Alfranca A, Martinez-Cruzado L, Tornin J, Abarrategi A, Amaral T, de Alava E, Menendez P, Garcia-Castro J and Rodriguez R. Bone microenvironment signals in osteosarcoma development. Cell Mol Life Sci 2015; 72: 3097-3113.
[32] He YZ, Liu YH, Cha N, Gao YW, Li F, Zhang M and Luan W. Exosomal circ_0048856 derived from non-small cell lung cancer contributes to aggressive cancer progression through down-regulation of miR-1287-5p. Pathol Res Pract 2022; 232: 153659.
[33] Luo YD, Liu L, Li XJ and Shi Y. Avasimibe inhibits the proliferation, migration and invasion of glioma cells by suppressing linc00339. Biomed Pharmacother 2020; 130: 110508.
[34] Xu GS, Li ML, Wu J, Qin CH, Tao Y and He HJ. Circular RNA circNRIP1 Sponges microRNA-138-5p to Maintain hypoxia-induced resis-

tance to 5-fluorouracil through HIF-1alpha-dependent glucose metabolism in gastric carcinoma. Cancer Manag Res 2020; 12: 2789-2802.
[35] Liu WH, Zhang JJ, Zou CY, Xie XB, Wang YQ, Wang B, Zhao ZQ, Tu J, Wang XS, Li HY, Shen JN and Yin JQ. Microarray expression profile and functional analysis of circular RNAs in osteosarcoma. Cell Physiol Biochem 2017; 43: 969-985.
[36] Wu YZ, Xie Z, Chen JX, Chen JX, Ni WY, Ma Y, Huang KM, Wang GL, Wang JY, Ma JJ, Shen SY and Fan SW. Circular RNA circTADA2A promotes osteosarcoma progression and metastasis by sponging miR-203a-3p and regulating CREB3 expression. Mol Cancer 2019; 18: 73.
[37] Chen JX, Liu G, Wu YZ, Ma JJ, Wu HF, Xie Z, Chen S, Yang YT, Wang SY, Shen PY, Fang YF, Fan SW, Shen SY and Fang XQ. Correction to: CircMYO10 promotes osteosarcoma progression by regulating miR-370-3p/RUVBL1 axis to enhance the transcriptional activity of beta-catenin/LEF1 complex via effects on chromatin remodeling. Mol Cancer 2020; 19: 75.
[38] Gui CP, Liao B, Luo CG, Chen YH, Tan L, Tang YM, Li JY, Hou Y, Song HD, Lin HS, Xu QH, Yao GS, Yao HH, Xi L, Luo JH, Cao JZ and Wei JH. circCHST15 is a novel prognostic biomarker that promotes clear cell renal cell carcinoma cell proliferation and metastasis through the miR-125a-5p/EIF4EBP1 axis. Mol Cancer 2021; 20: 169.
[39] Jiang T, Wang HY, Liu LY, Song H, Zhang Y, Wang JQ, Liu L, Xu T, Fan RZ, Xu YX, Wang S, Shi LS, Zheng L, Wang RH and Song J. CircIL4R activates the PI3K/AKT signaling pathway via the miR-761/TRIM29/PHLPP1 axis and promotes proliferation and metastasis in colorectal cancer. Mol Cancer 2021; 20: 167.
[40] Yu YZ, Lv DJ, Wang C, Song XL, Xie T, Wang T, Li ZM, Guo JD, Fu DJ, Li KJ, Wu DL, Chan FL, Feng NH, Chen ZS and Zhao SC. Hsa_circ_0003258 promotes prostate cancer metastasis by complexing with IGF2BP3 and sponging miR-653-5p. Mol Cancer 2022; 21: 12.
[41] Harris MA and Hawkins CJ. Recent and ongoing research into metastatic osteosarcoma treatments. Int J Mol Sci 2022; 23: 3817.
[42] Kristensen LS, Jakobsen T, Hager H and Kjems J. The emerging roles of circRNAs in cancer and oncology. Nat Rev Clin Oncol 2022; 19: 188-206.
[43] Liu C, Ge HM, Liu BH, Dong R, Shan K, Chen X, Yao MD, Li XM, Yao J, Zhou RM, Zhang SJ, Jiang Q, Zhao C and Yan B. Targeting pericyte-endothelial cell crosstalk by circular RNA-cPWWP2A inhibition aggravates diabetes-induced microvascular dysfunction. Proc Natl Acad Sci U S A 2019; 116: 7455-7464.
[44] Chen QJJ, Wang HB, Li Z, Li FW, Liang LL, Zou YR, Shen H, Li J, Xia Y, Cheng ZJ, Yang T, Wang K and Shen F. Circular RNA ACTN4 promotes intrahepatic cholangiocarcinoma progression by recruiting YBX1 to initiate FZD7 transcription. J Hepatol 2022; 76: 135-147.
[45] Shen SY, Wu YZ, Chen JX, Xie Z, Huang KM, Wang GJ, Yang YT, Ni WY, Chen ZJ, Shi PH, Ma Y and Fan SW. CircSERPINE2 protects against osteoarthritis by targeting miR-1271 and ETS-related gene. Ann Rheum Dis 2019; 78: 826-836.
[46] Weng WH, Wei Q, Toden S, Yoshida K, Nagasaka T, Fujiwara T, Cai SJ, Qin HL, Ma YL and Goel A. Circular RNA ciRS-7-A promising prognostic biomarker and a potential therapeutic target in colorectal cancer. Clin Cancer Res 2017; 23: 3918-3928.
[47] Kristensen LS, Ebbesen KK, Sokol M, Jakobsen T, Korsgaard U, Eriksen AC, Hansen TB, Kjems J and Hager H. Spatial expression analyses of the putative oncogene ciRS-7 in cancer reshape the microRNA sponge theory. Nat Commun 2020; 11: 4551.
[48] Peng FF, Gong WQ, Li ST, Yin BH, Zhao C, Liu WT, Chen XW, Luo CW, Huang QY, Chen T, Sun LZ, Fang S, Zhou WD, Li ZJ and Long HB. circRNA_010383 Acts as a sponge for miR-135a, and its downregulated expression contributes to renal fibrosis in diabetic nephropathy. Diabetes 2021; 70: 603-615.
[49] Xiang Q, Kang L, Wang JT, Liao ZW, Song Y, Zhao KC, Wang K, Yang C and Zhang YK. CircRNA-CIDN mitigated compression loading-induced damage in human nucleus pulposus cells via miR-34a-5p/SIRT1 axis. EBioMedicine 2020; 53: 102679.
[50] Qi HY, Chi L, Wang XG, Jin X, Wang WS and Lan JP. Identification of a seven-lncRNA-mRNA signature for recurrence and prognostic prediction in relapsed acute lymphoblastic leukemia based on WGCNA and LASSO analyses. Anal Cell Pathol (Amst) 2021; 2021: 6692022.
[51] Xu YL, Yang Y, Cai YY, Liu F, Liu YL, Zhu Y and Wu JG. The X protein of hepatitis B virus activates hepatoma cell proliferation through repressing melanoma inhibitory activity 2 gene. Biochem Biophys Res Commun 2011; 416: 379-384.